TRIUMF

Advances in β-NMR @ ISAC

Sarah Dunsiger
Centre for Molecular and Materials Science, TRIUMF

21 August 2019

Comparison of Spin Resonance Techniques

	NMR	Bulk μSR 8Li βNMR
Polarisation	**<0.1**	**>0.8**
Detection	**Electronic pickup**	**Anisotropic β decay**
Sensitivity	**10^{17} spins**	**10^{7} spins**
T_1 range (s)	**10^{-5}-10^{2}**	**10^{-8}-10^{-4} 10^{-3}-10^{3}**
Range	**0.5 mm**	**10-3000 Angstroms**

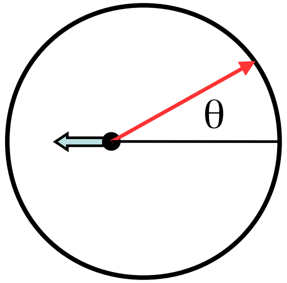

$^{8}Li^{+} \rightarrow \; ^{8}Be^{2+} + e^{-} + \nu_e$

Lifetime=1.2 s

$SrTiO_3$: the Prototypical Perovskite

W A MacFarlane et al, Physica B 326, 209 (2003)

Cubic – tetragonal structural Phase transition ~ 105 K
Quantum Paraelectric below ~ 4K

Structural information from 8Li S=2 nuclear spin probe at inequivalent face centre sites

$$\nu_{m\leftrightarrow m-1}|_{m=-1\cdots 2} = \nu_0 - \frac{\nu_Q}{2}\left(m-\frac{1}{2}\right)[3\cos^2(\theta)-1]$$

ν_Q(211 K) = 153 kHz

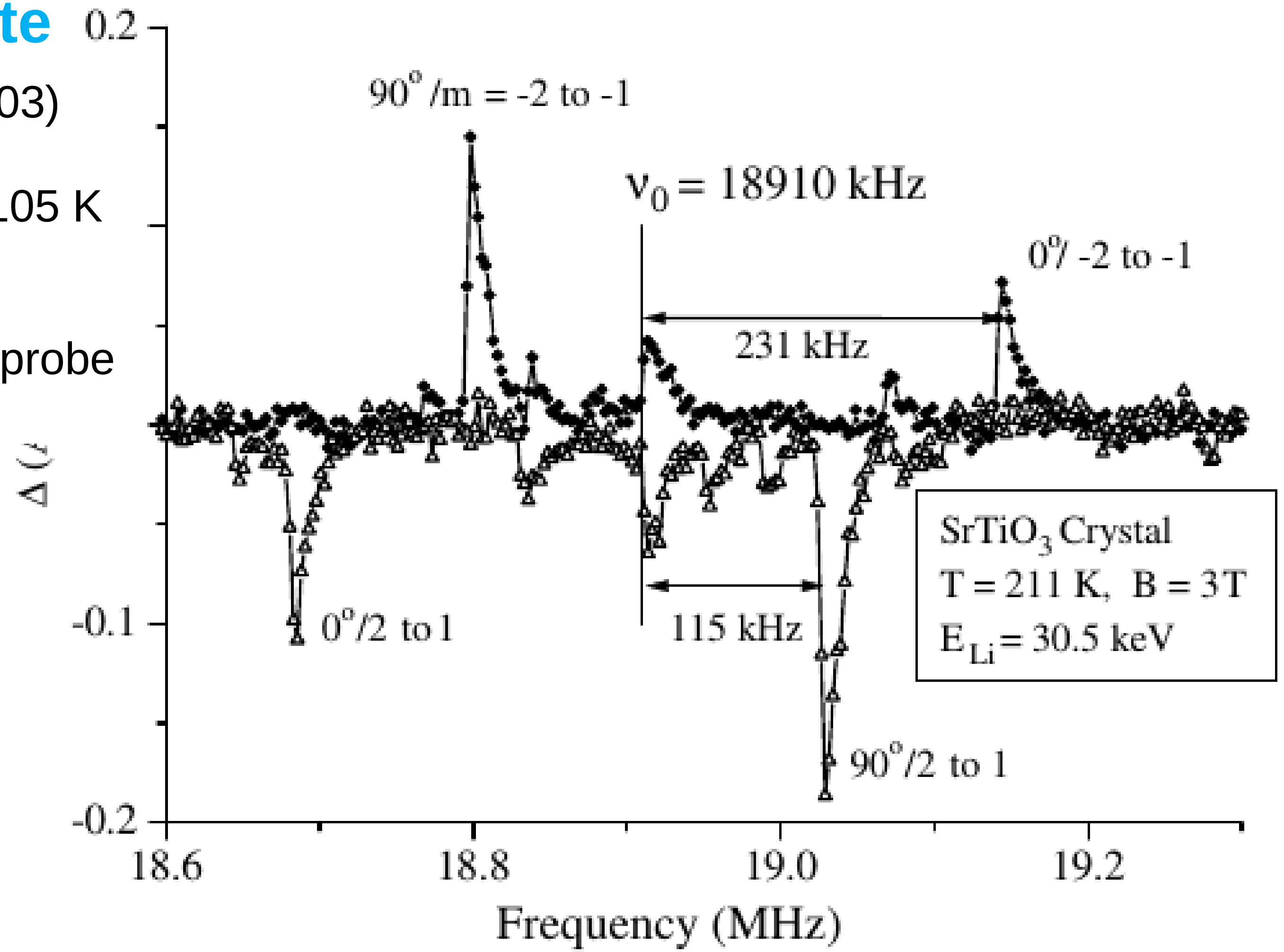

$\nu_Q=e^2qQ/4h$; Q is the nuclear electric quadrupole moment; θ the angle between the applied magnetic field and the symmetry axis of the EFG tensor, assuming the EFG is cylindrically symmetric

Determination of the nature of fluctuations

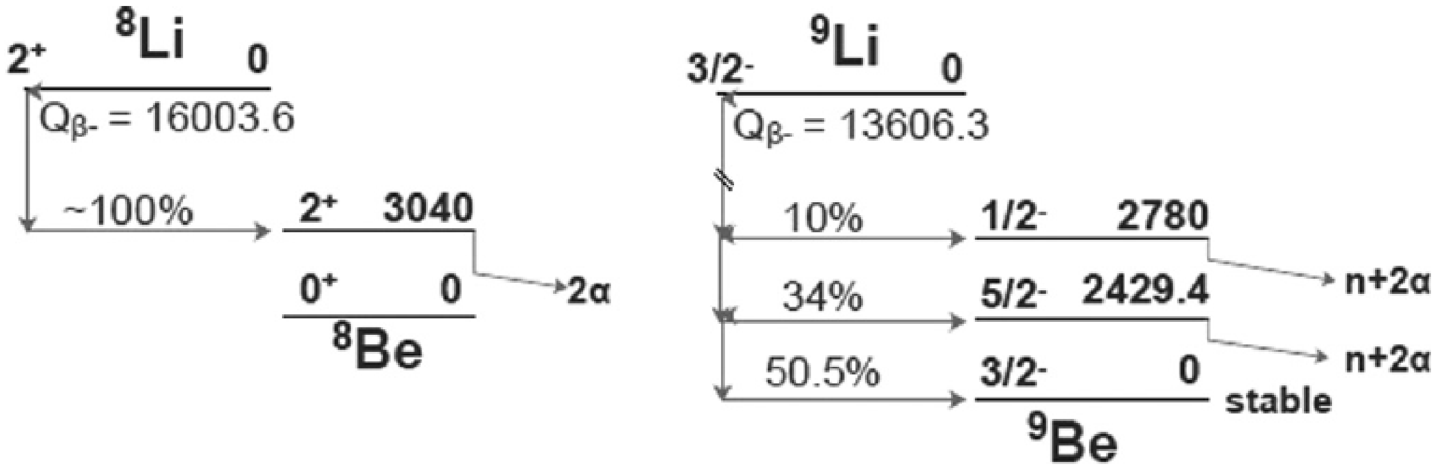

Asy=-1
3/5
-2/5

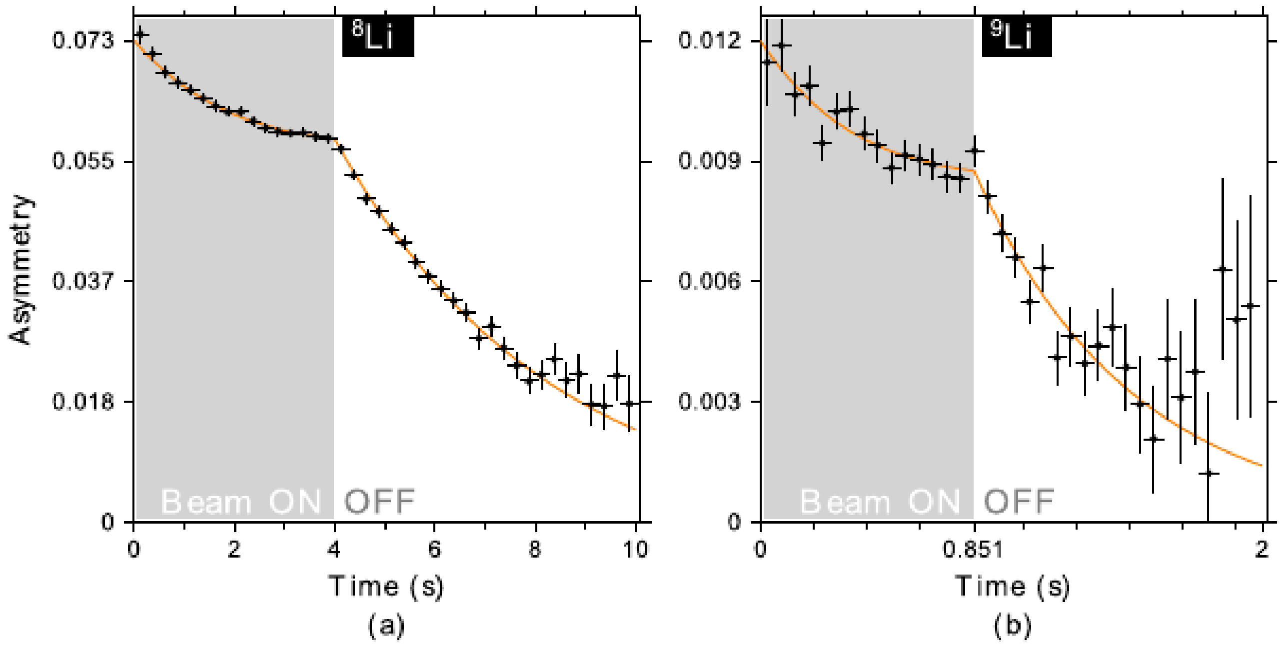

Long pulse spectra in Pt foil
18 keV at 300 K under 6.55 T

A Chatzichristos et al,
Phys Rev B 96, 014307 (2017)

Magnetic and Quadrupolar Limits : Pt and $SrTiO_3$

$$R(I,I') \equiv \frac{1/T_1(I)}{1/T_1(I')} = \frac{1/T_1^{\mathrm{M}}(I) + 1/T_1^{\mathrm{Q}}(I)}{1/T_1^{\mathrm{M}}(I') + 1/T_1^{\mathrm{Q}}(I')}$$

$$R_{\mathrm{M}}(I,I') = \left(\frac{\mu/I}{\mu'/I'}\right)^2 = \left(\frac{\gamma}{\gamma'}\right)^2$$

Pt: Korringa relaxation from magnetic hyperfine interaction between the nuclear spin and the spin of the conduction electrons

$$R_{\mathrm{Q}}(I,I') = \frac{f(I)}{f(I')}\left(\frac{Q}{Q'}\right)^2$$

$SrTiO_3$: quadrupolar fluctuations in Electric Field Gradient

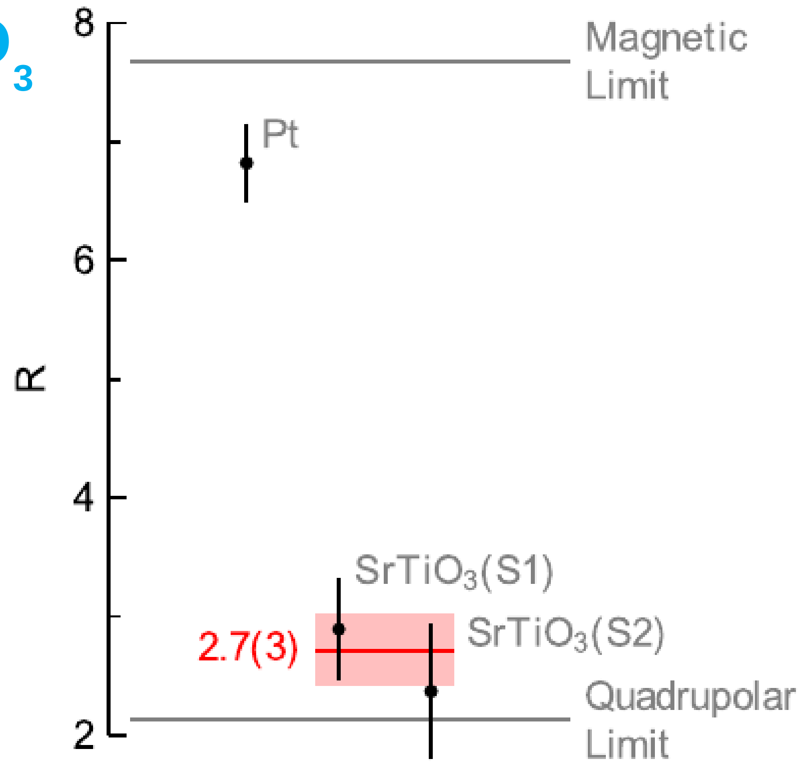

	I^π	τ_β (s)	μ (μ_N)[a]	Q (mb)[b]
^{8}Li	2^+	1.2096(5) [14]	+1.653560(18) [15]	+32.6(5) [16]
^{9}Li	$3/2^-$	0.2572(6) [17]	+3.43678(6) [15]	−31.5(5) [16]

A Chatzichristos et al, Phys Rev B 96, 014307 (2017)

Tracer diffusion and surface trapping of 8Li+ in rutile TiO_2

A Chatzichristos et al, accepted for Phys Rev Lett (2019)

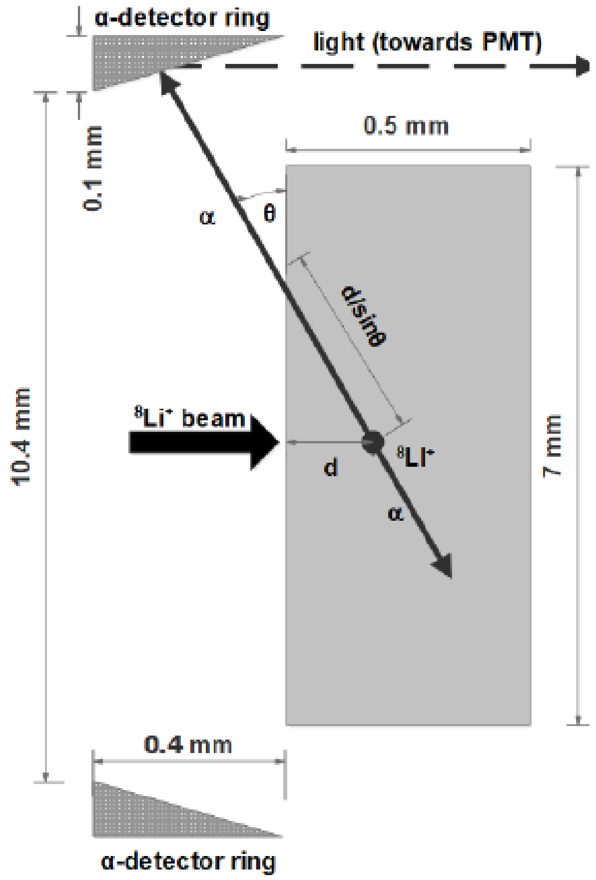

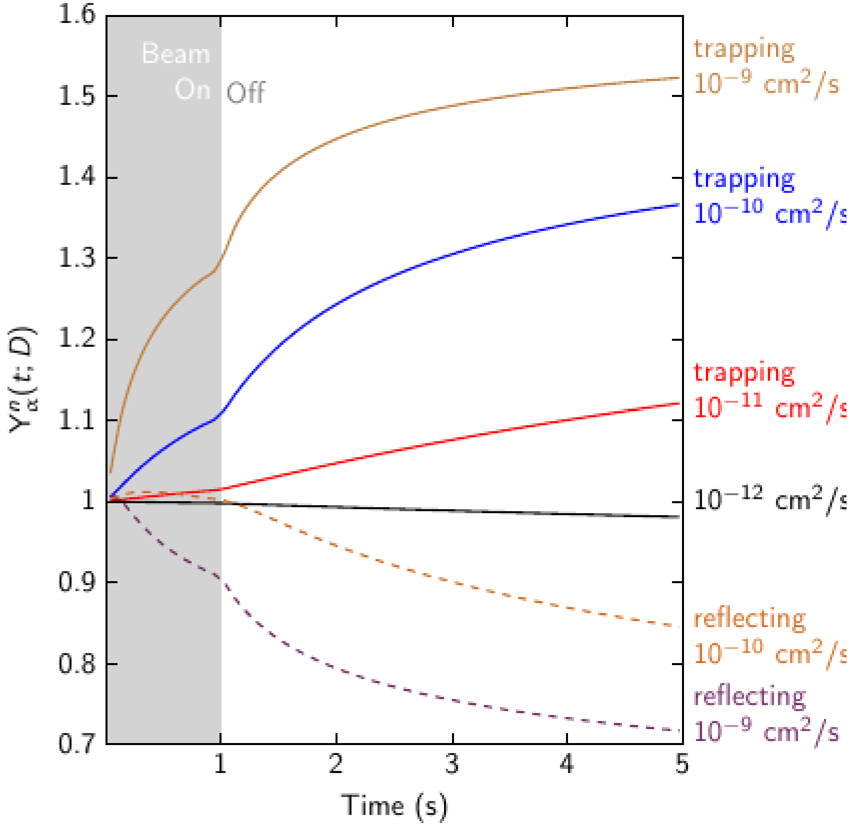

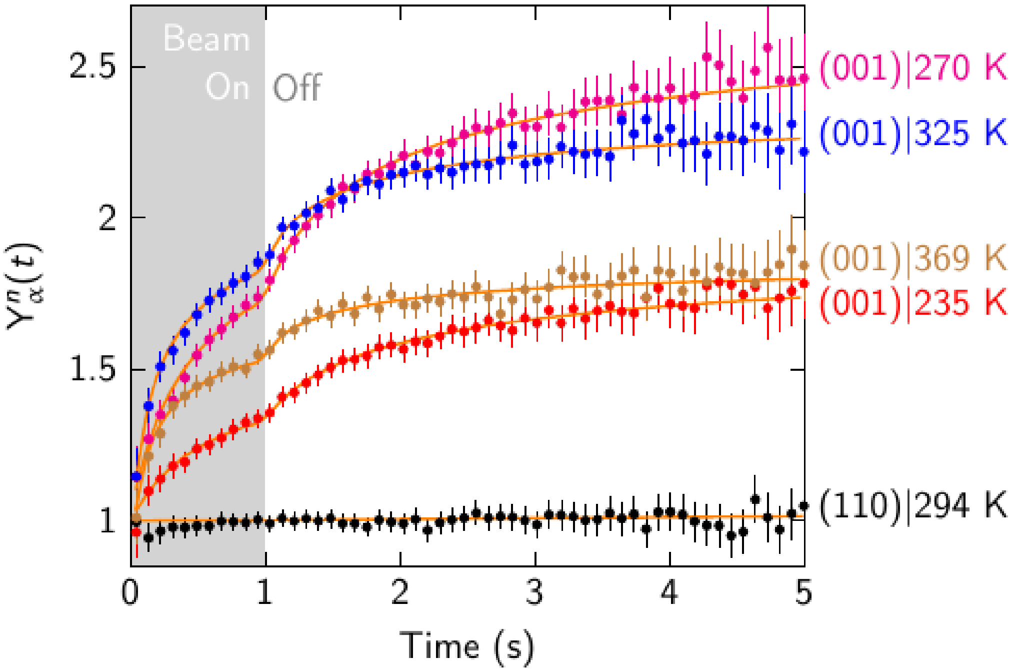

Simulated (using GEANT4) normalized α-yield as a function of time $Y=N_\alpha/N_\beta$ (t; D) in TiO_2, given an initial beam energy of 25 keV, dependent on both the diffusion rate and the surface boundary condition.

TRIUMF

Upgrades to NQR Spectrometer

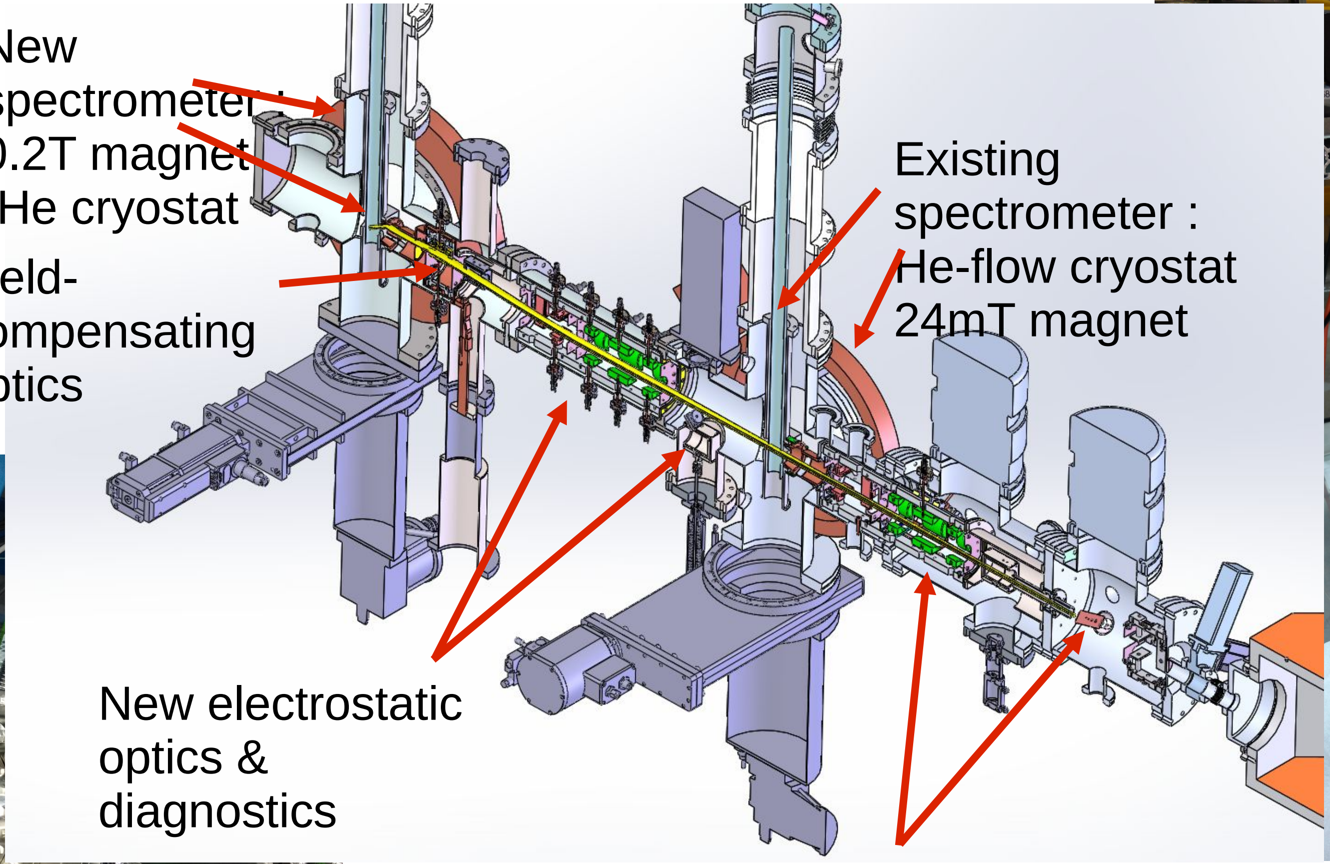

New spectrometer : 0.2T magnet ^{3}He cryostat

Field-compensating optics

Existing spectrometer : He-flow cryostat 24mT magnet

New electrostatic optics & diagnostics

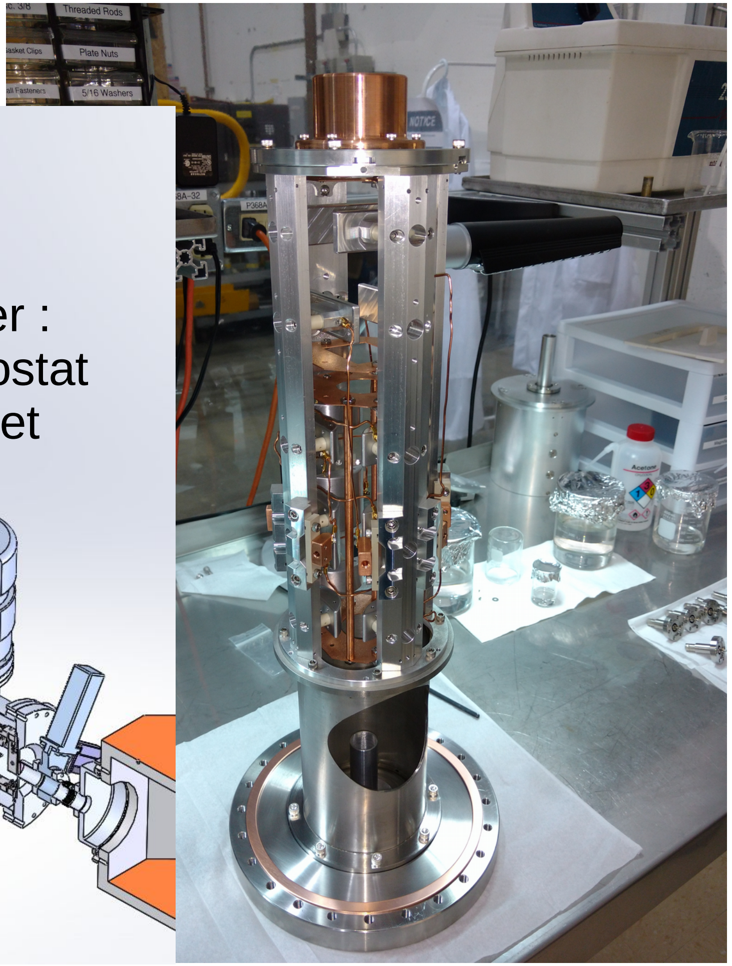

Improved electrostatic optics & diagnostics

Beam Optics calculations

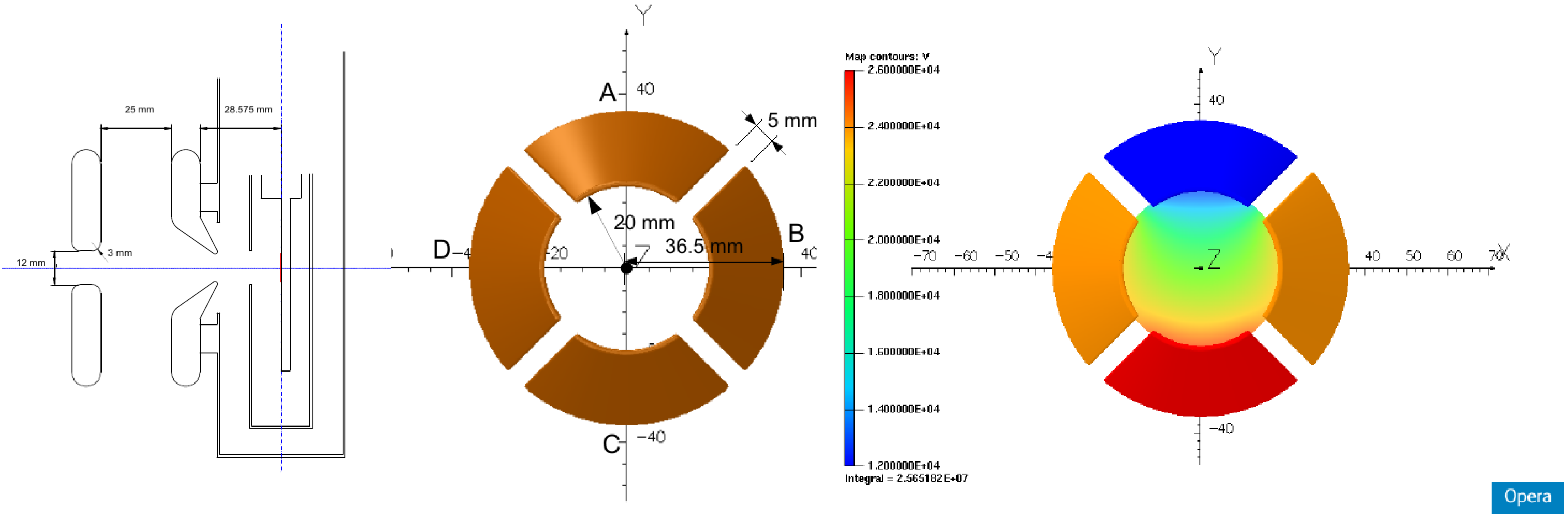

Calculated potential contour in the XY plane (at the decelerator exit, z = 0.3 m) for a typical applied potentials of 12 kV (A), 24 kV (B & D) and 26 kV (C) to the decelerator electrodes. S Saminathan

Beam Optics calculations – the Silver Lining

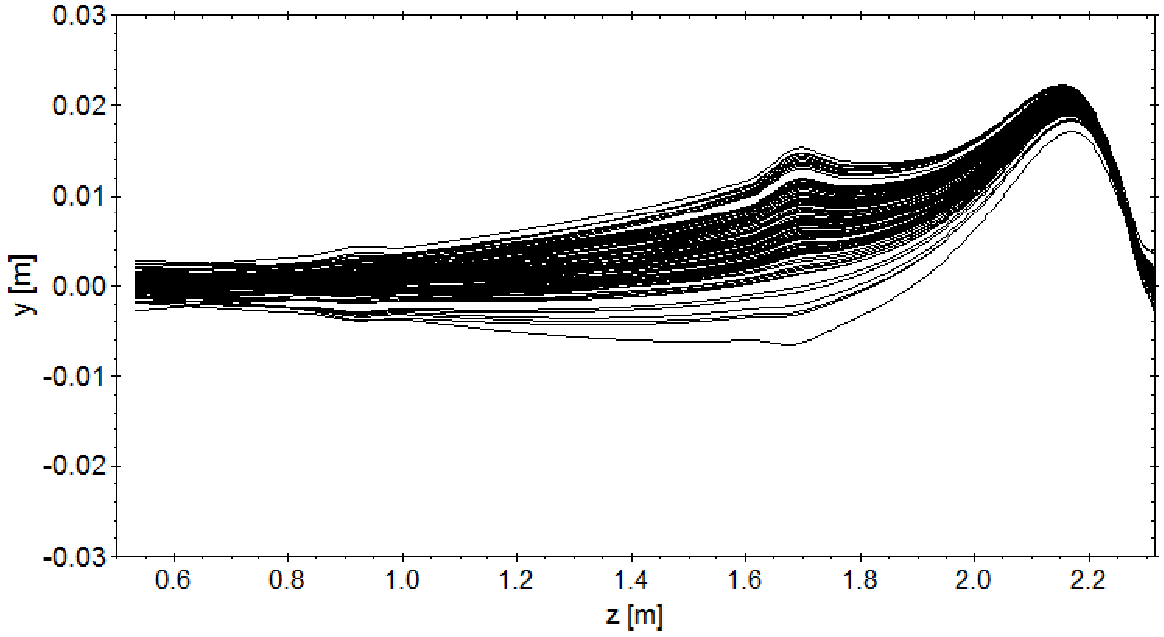

Calculated ion trajectories of 28 keV 8Li+ beam in ZY-plane at 0.2 Tesla

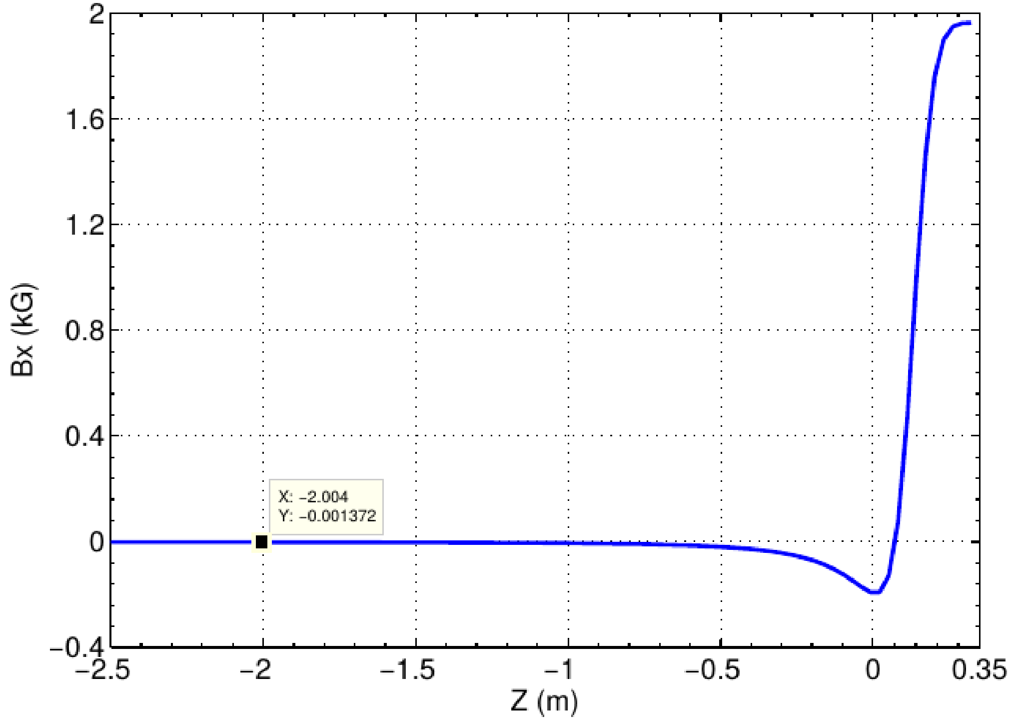

Calculated magnetic field along the beam axis for planned Helmholtz coil. Sample at z = 0.322 m

Magnetic flux entry measured with muon spin rotation

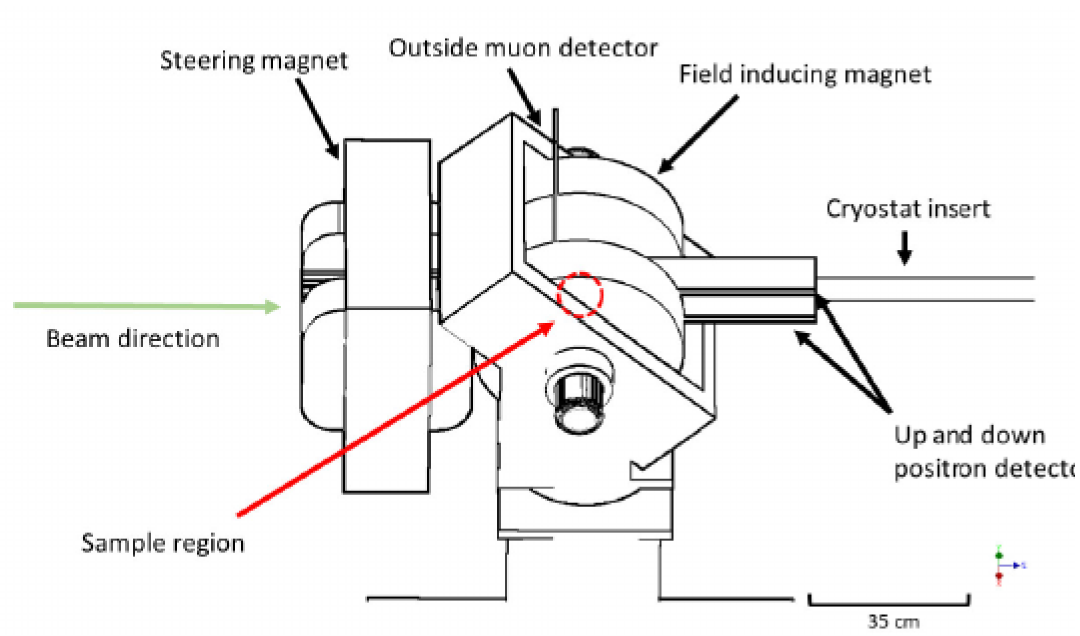

Hodge-Podge spectrometer,
named for its recycled components

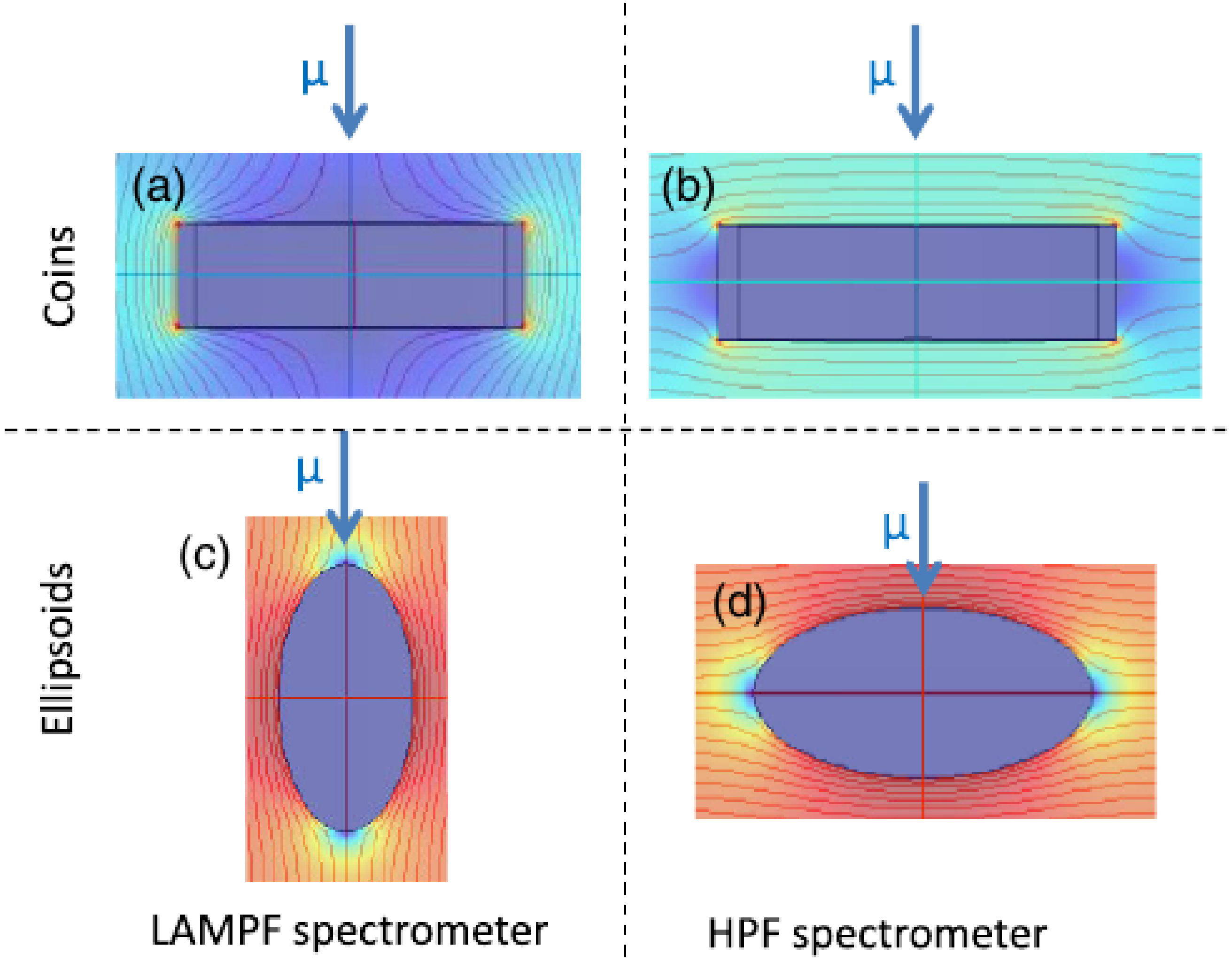

T Junginger et al, Phys Rev Accel and Beams 21, 032002 (2018)

β-NMR Resonances in Bi, Sb and Topological Insulator $Bi_{0.9}Sb_{0.1}$

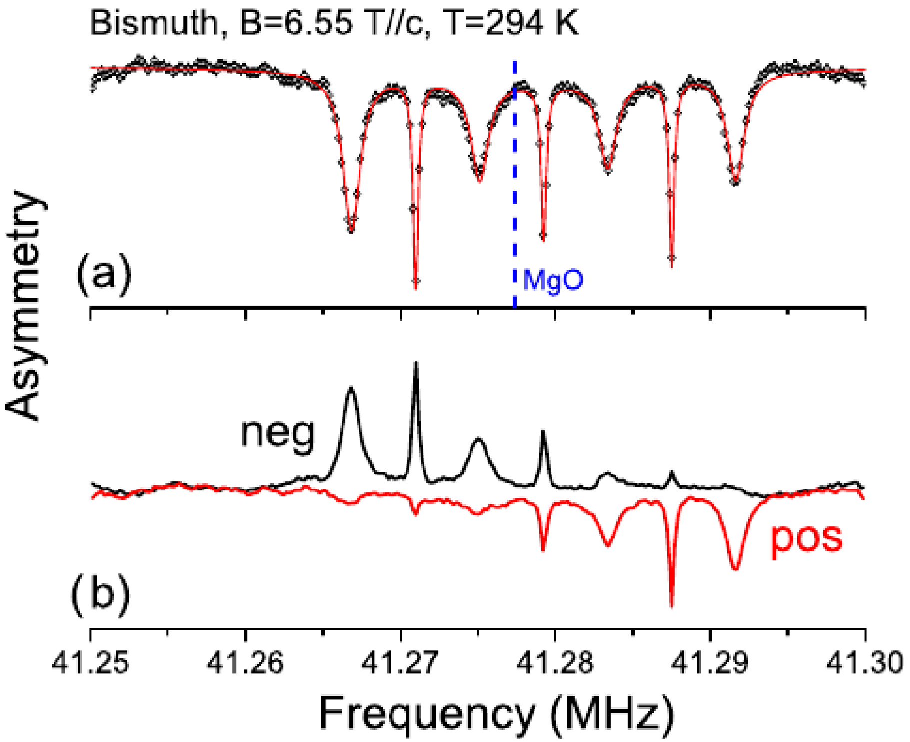

W A MacFarlane et al, Phys Rev B 90, 214422 (2014)

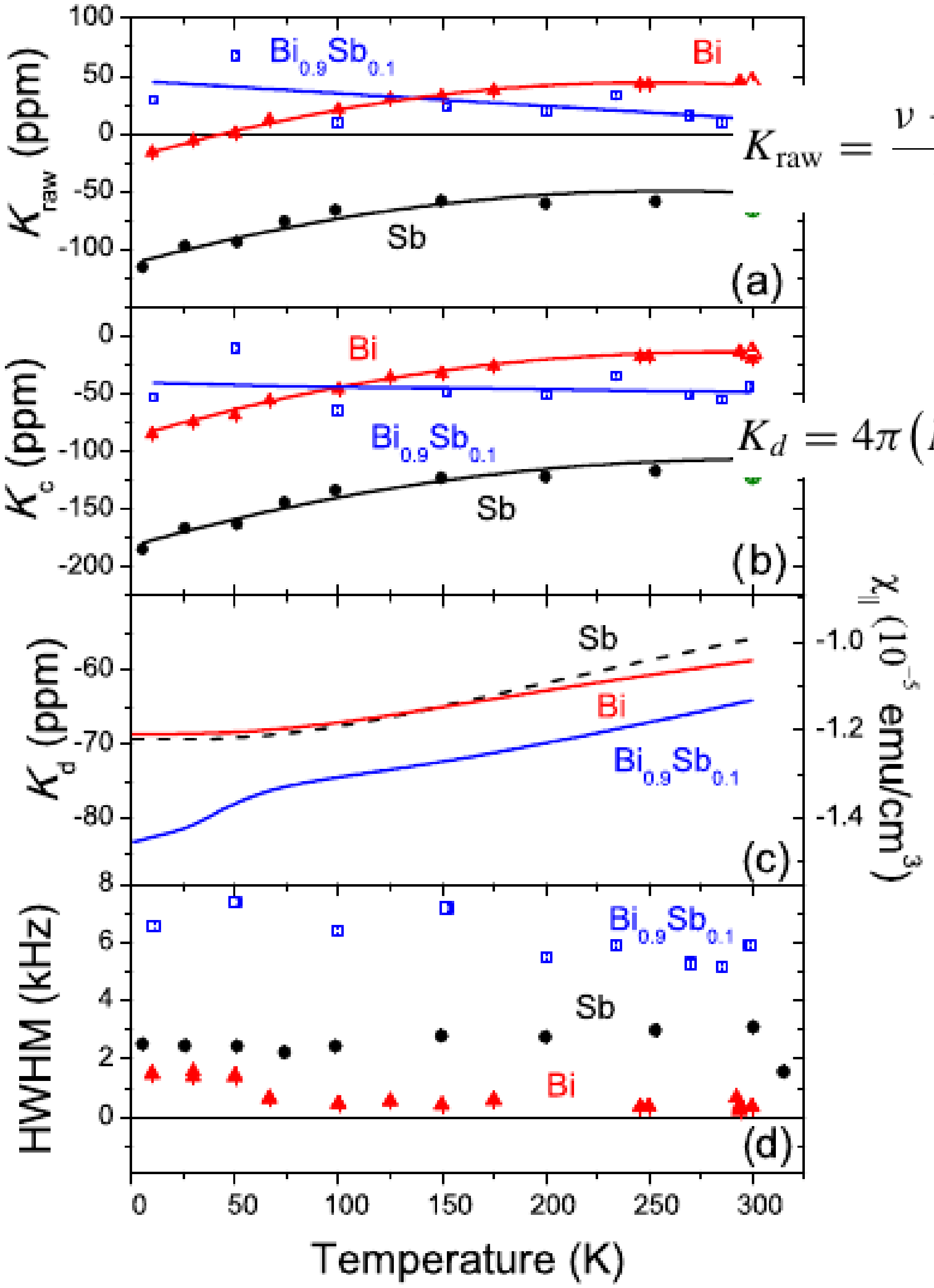

$$K_{\text{raw}} = \frac{\nu - \nu_{\text{MgO}}}{\nu_{\text{MgO}}}$$

$$K_d = 4\pi\left(N - \tfrac{1}{3}\right)\chi$$

WURST Frequency Swept β-NMR Technique

Magnetisation trajectory

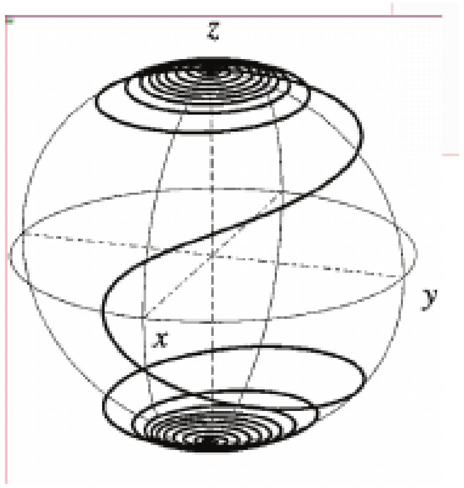

A means to utilise Wideband, Uniform Rate, Smooth Truncation RF pulses to extract frequency spectra as a function of T1 relaxation time in a single pulsed beam scan. This is also very efficient way to collect spectral data since the beam can be shared.

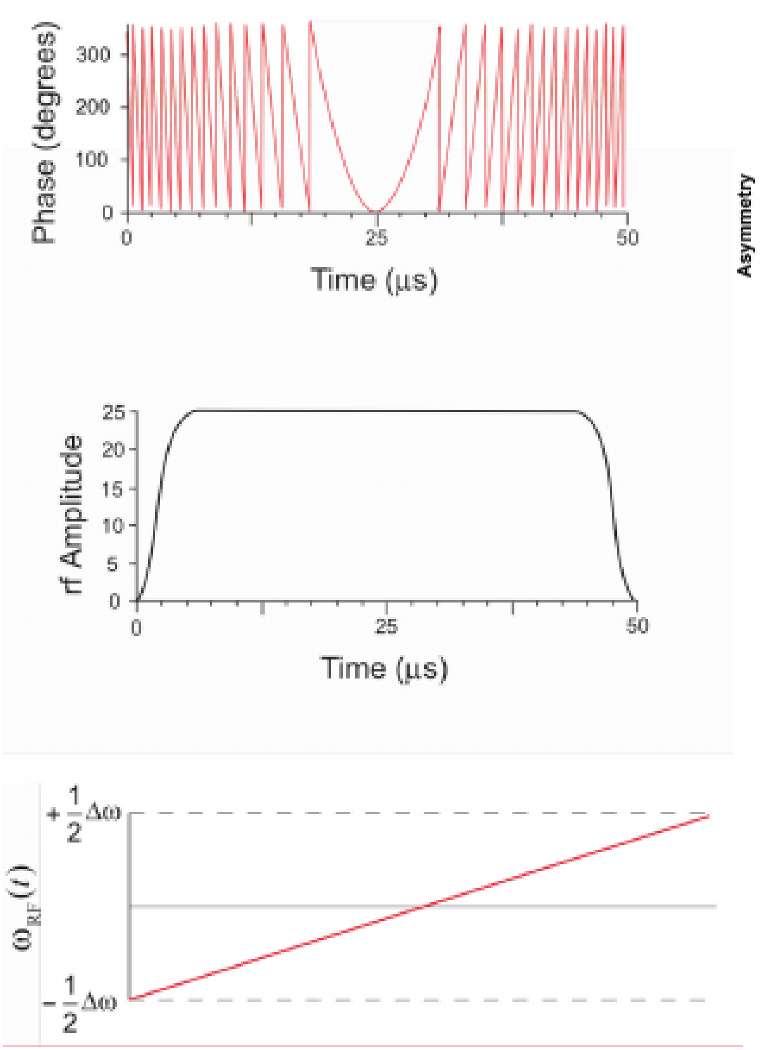

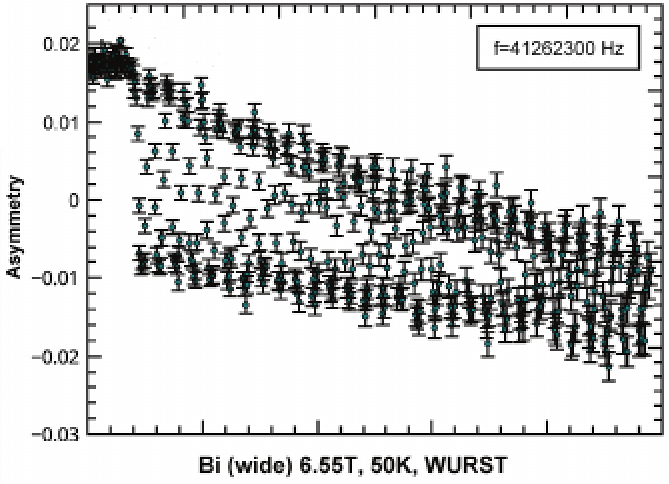

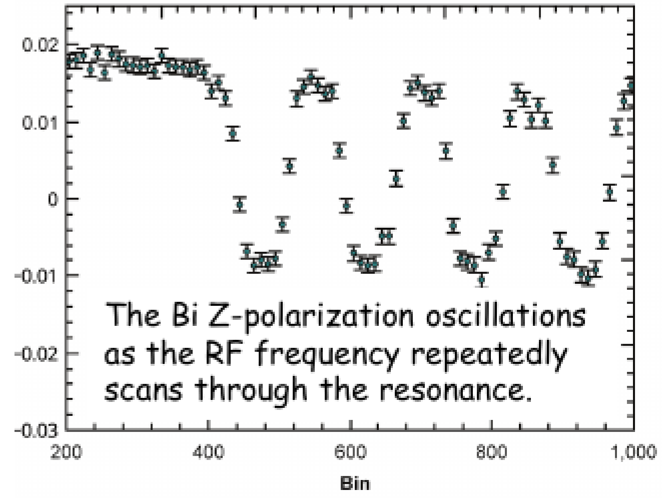

The a) phase, b) amplitude and c) frequency of the WURST RF pulse.

TRIUMF

Structural Phase Transitions in Perovskites ABO_3

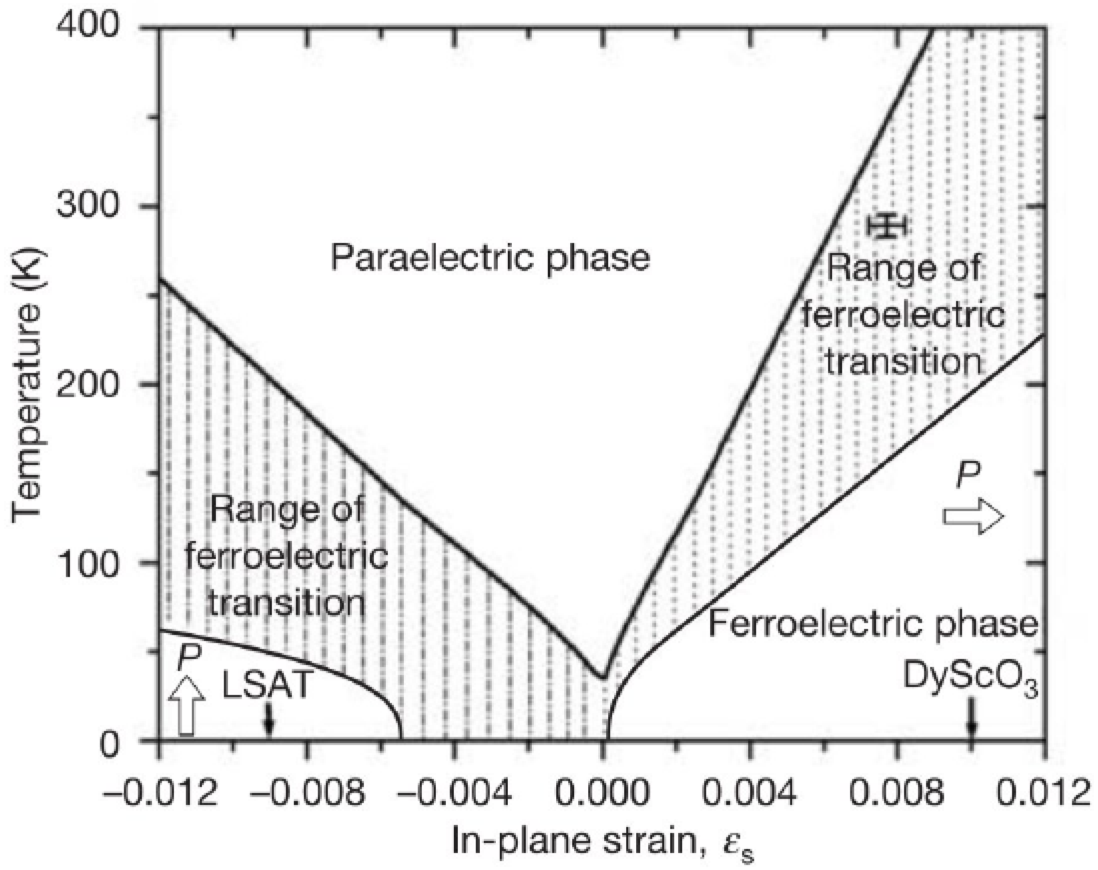

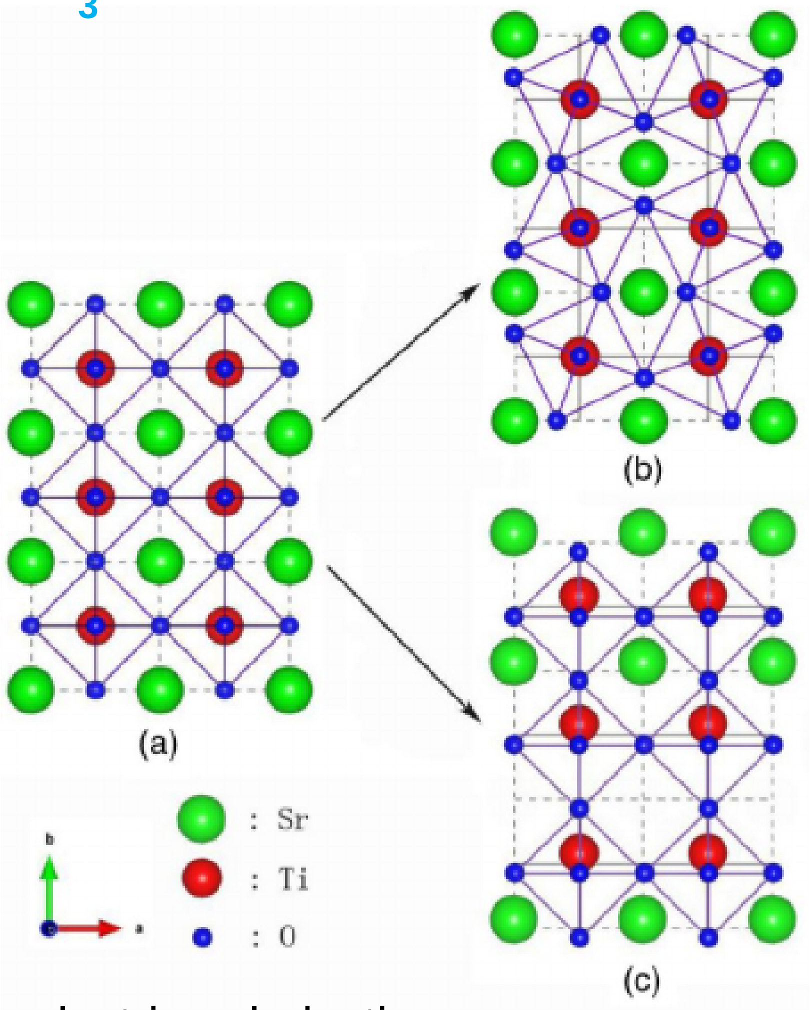

LHS) Phase diagram of epitaxially grown $SrTiO_3$ on substrates with different lattice mismatches. Arrows indicate direction of ferroelectric polarization

RHS) Possible $SrTiO_3$ crystal structures: (a) cubic (undistorted) phase (b) anti-ferrodistortive oxygen octahedra rotation cause distortions (c) polar, ferroelectric distortion

Advancement in RF techniques: RF comb

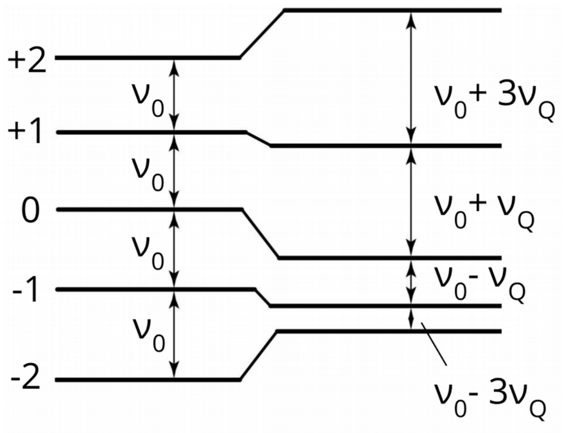

Simultaneous excitation of all transitions

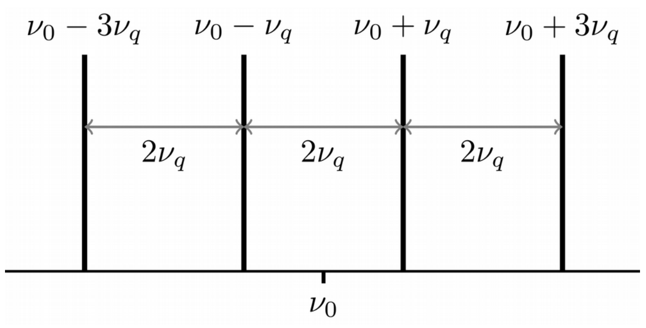

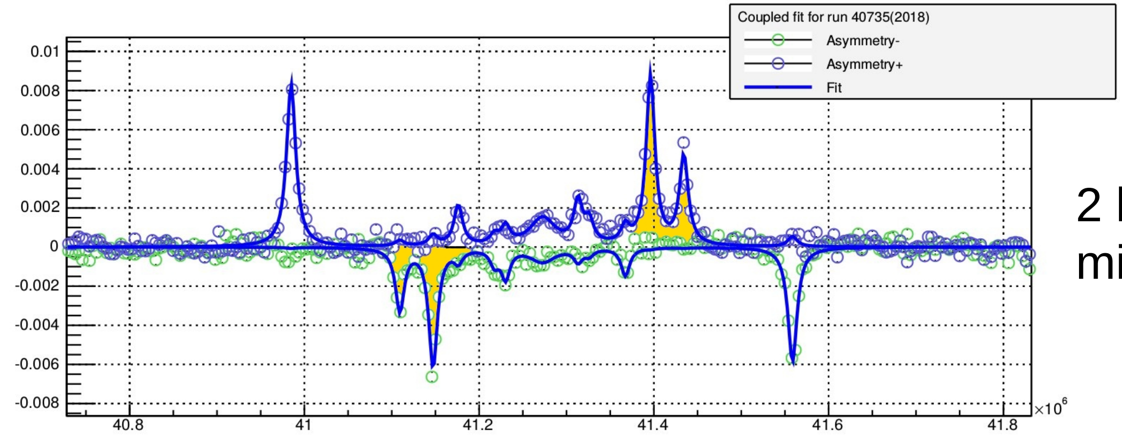

2 hours 40 minutes

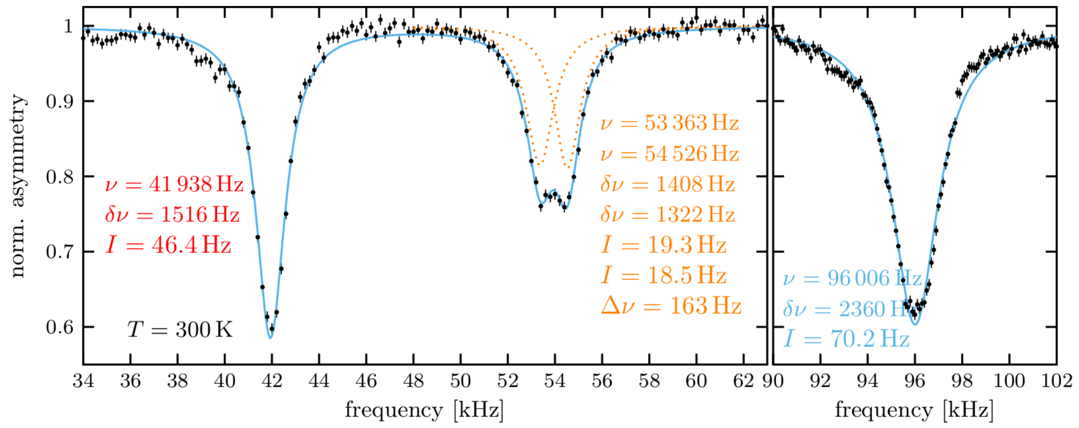

34 minutes

$LaAlO_3$ T=300 K

TRIUMF

25Mg NMR vs 31Mg β-NMR in Ionic Liquids

1-ethyl-3-methylimidazolium acetate and
1-ethyl-3-methylimidazolium Dicyanamide

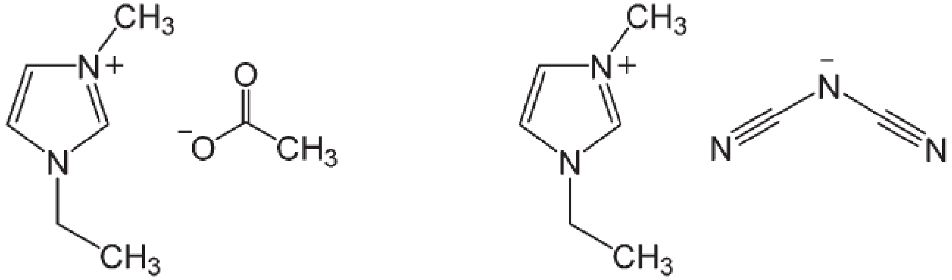

[Mg(DCA)6]4− (−60.2 ppm),
[Mg(DCA)5(H2O)]3− (−52.0 ppm),
[Mg(DCA)4(H2O)2]2− (−43.2 ppm)

[Mg(Ac)4(H2O)2]2− (−38.1 ppm),
[Mg(Ac)2(H2O) 4] (−31.9 ppm)

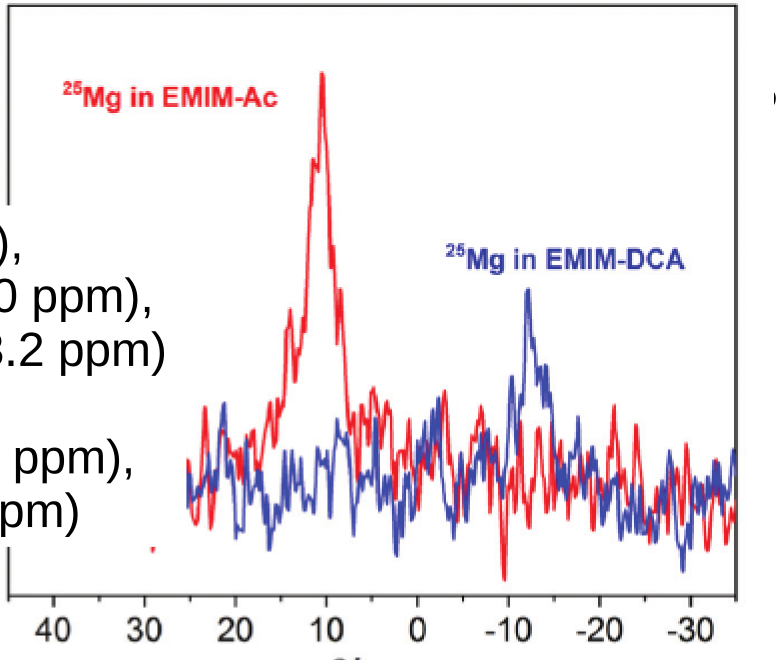

D Szunyogh et al, Dalton Trans. 47, 14431 (2018)

	β-NMR	NMR
No. Mg ions	~ $2 \cdot 10^{8}$	~ 10^{18}
Spin	1/2	5/2
Volume	2 - 4 μL	550 μL
Temp	295 K	345 K
Mag. field	3.41 T	11.7 T
Exp. time	1-2 h	~24 h

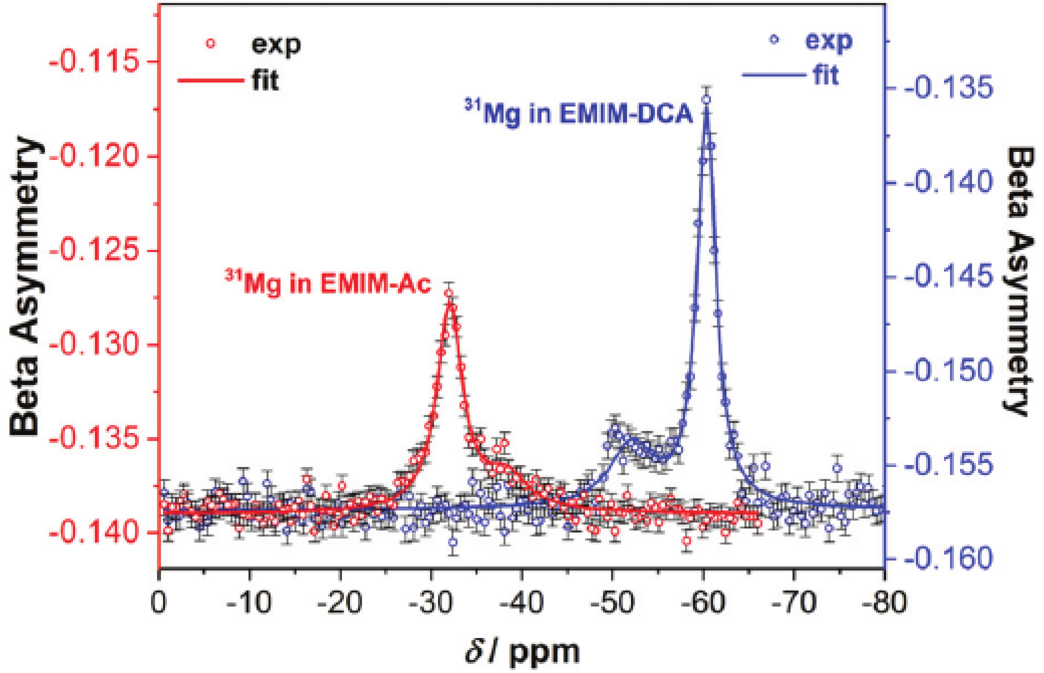

25 mM MgCl2 in EMIM-Ac (red) and EMIM-DCA (blue)

β-NMR of Biologically Relevant Complexes

- Probe site coordination geometry: types, number and geometric arrangement of coordinating atoms
- Allow for experiments at physiologically relevant concentrations

Pressure distribution simulated using Molflow+ (E Kallenberg)

Ideal pinhole arrangement for transmission + pressure: (Target)

3mm – 4mm – 4mm (Beamline)

- Probe site dynamics on a ms timescale (exchange dynamics, molecular reorientational correlation times)

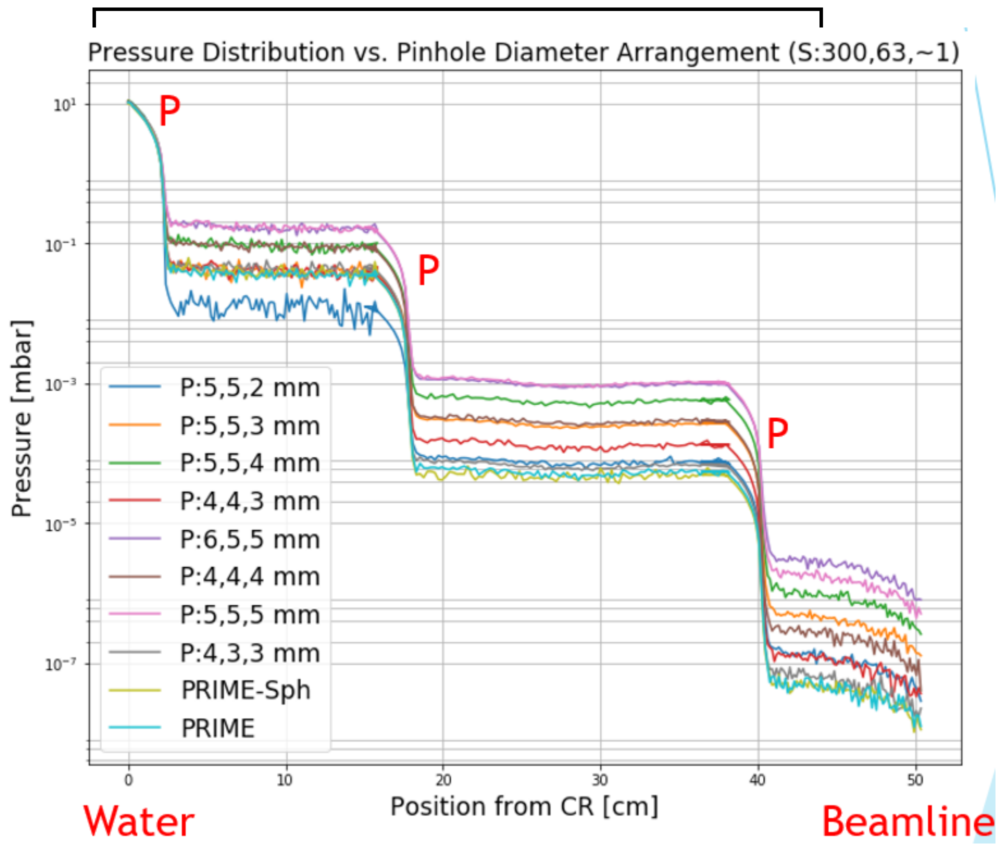

Isotope	Half-life [s]	Spin	Decay mode	Magnetic moment [u_N]	Quadruple moment [b]	Yields [1/s]
^{230}Ac	122	+1	β^- (100%)	unknown	unknown	$3\cdot10^4$ *
^{232}Ac	119	(+1)	β^- (100%)	unknown	unknown	$1\cdot10^4$ *

* The provided yields were measured using Re surface ion source. Yields of e.g. ^{225}Ac measured in Dec 2016 and Sep 2018 showed, however, an order of magnitude increase in yields when using TRILIS. This enhancement has also been showed for other measured isotopes.

Proposed Layout in ISAC-1 Hall

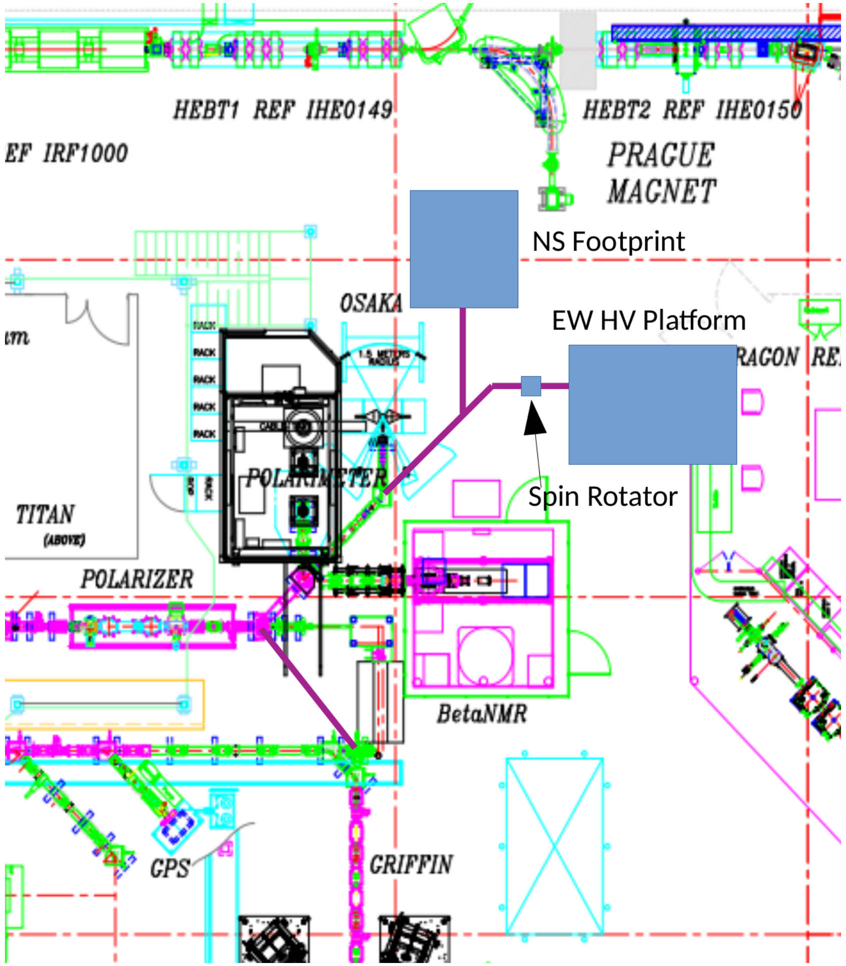

OSAKA Life Science and Nuclear Physics
dedicated β-NMR spectrometer for liquids and high vapour pressure applications, focussing on systems of biochemical and medical relevance; chemical Shift Measurements by ^{31}Mg, ^{54}Cu, ^{74}Cu, ^{75}Cu, ^{230}Ac, ^{232}Ac β-NMR

NSP Nuclear Structure and Symmetry
2x2.5 m footprint for modular experiments including resonant ionisation decay-spectroscopy; development of spin-polarised ^{32}Na beam; test of Time Reversal Symmetry Using Polarised Unstable Nuclei

EWP Physical Science
dedicated 2.5x3 m high voltage platform, 0.1-30 keV ions
radio frequency spin echo and adiabatic inversion techniques
vector magnet (0-2 Tesla || beam, 0-0.5 Tesla ⊥ beam)
4-400 K cryo-oven
pencil beam spot for investigation on 200 μm lateral length scale

GRIFFIN Nuclear Structure and Symmetry
3 m low energy polarised beam transport

POLARIZER beamline and Laser Upgrade

Rapid Switching of Beam and Helicity
Quasi continuous Beam on Three Channels

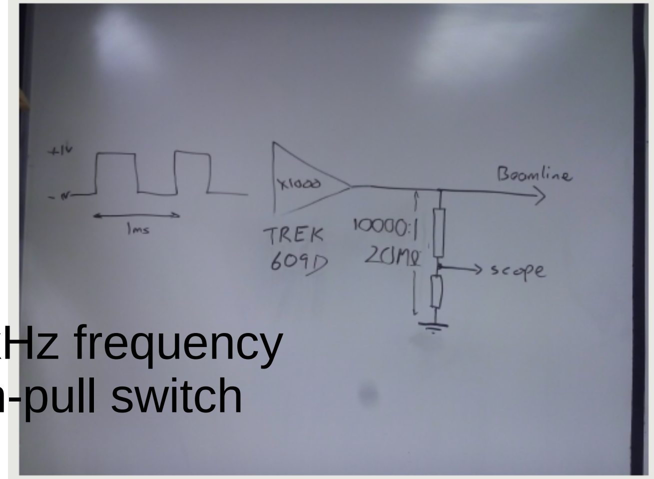

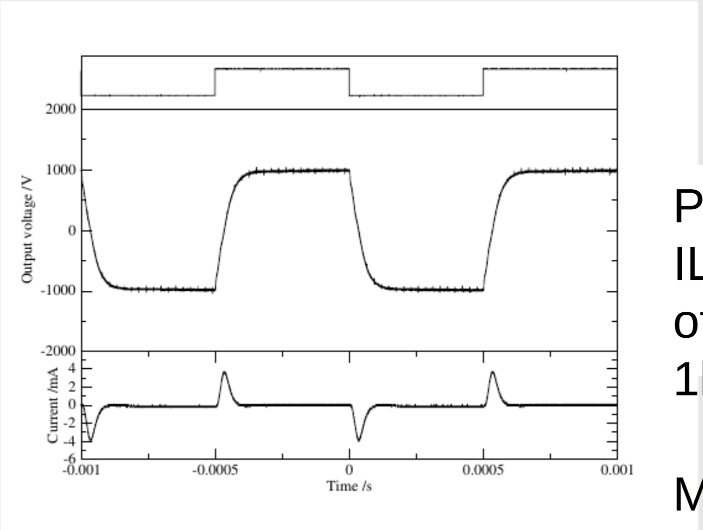

Rapid switching at kHz frequency
using Trek HV push-pull switch

Kerr cell: birefringence under application of electric field ($\Delta n = \lambda K E^2$)

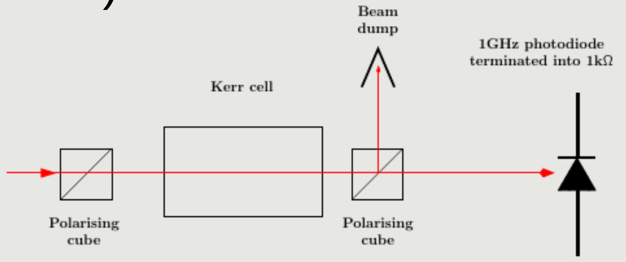

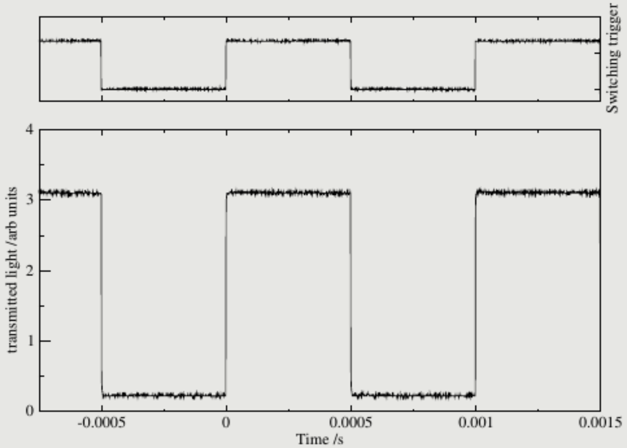

Proposed set-up identical to ILT:YCB3 plates into and out of TITAN. Routine pulsing at > 1kHz with 50:50 duty cycle

M Pearson

TRIUMF

Summary

Advancements in :

1) Radiofrequency techniques, to bring all the power of conventional NMR in spin manipulation to β-NMR, a depth resolved variant.

2) Sample environment (3He system; new spectrometers are being proposed, including pixelated Si photomultiplier detectors)

3) Multiplexing the incoming polarised radioactive isotope beam to take full advantage of increased availability once ARIEL comes online.

^{8}Li Spin Lattice Relaxation in Bi, Sb and $Bi_{0.9}Sb_{0.1}$

Importance of orbital interactions 3D Dirac electron systems:

- μ inside the band gap, $T_1^{-1} \sim T^3 \log(2T/\omega_0)$ for temperatures > band gap, (ω_0 nuclear Larmor frequency; μ chemical potential)
- μ in the conduction or valence bands, $T_1^{-1} \propto T k_F^2 \log(2 v_F k_F/\omega_0)$ for low temperatures, (k_F and v_F Fermi momentum and velocity).
- K_{orb} is negative and its magnitude significantly increases with decreasing temperature when μ is located in the band gap.
- Korringa relation does not hold in the Dirac electron systems

T Hirosawa et al, J Phys Soc Jpn 86, 063705 (2017)
H Maebashi et al, J Phys Chem Solids (2017) (in press)